Icebreaking Ability of a Free-rising Buoyant Sphere

B. Y. Ni [a*]; H. Tan [a]; Yu. A. Semenov [a]; C. X. Zhang [a]
a. College of Shipbuilding Engineering, Harbin Engineering University, Harbin, China;
*nibaoyu@hrbeu.edu.cn

HIGHLIGHTS

- It is found that the damage degree of the ice plate depends on the kinetic energy of a free-rising buoyant sphere at the moment of collision, instead of momentum.
- Some simplified theoretical approaches are adopted to find an explicit expression of the optimal relative density $\bar{\rho}_{op}$ of the sphere under different initial submergence depth. It is found for a non-viscous case, $\bar{\rho}_{op}$ equals to $\frac{\sqrt{3}-1}{2}$ always.

1 INTRODUCTION

Vertical icebreaking is common in nature. For example, a bowhead whale needs to break the ice sheet above it for ventilation and it can break an ice sheet up to 60cm thick by buoyance [1]. Therefore, many scholars have studied icebreaking of a body moving in the vertical direction. Ren and Zhao [2] studied the process of a sphere falling from the top of an ice plate, and breaking ice before entering the water. Wang et al. [3] simulated the process of an underwater cylinder breaking ice vertically before exiting the water. Ye et al. [4] simulated submarine surfacing through the ice under a given constant speed by using the peridynamics method. Orlov and Bogomolov [5] quantitatively described the process of large impactors penetrating ice in the initial range below the speed of sound in air.

It can be seen that most previous work on the collision of a body and ice along vertical direction either concerned the intrusion of the sphere into the thick ice, or the damage of ice under the body with a prescribed velocity. To our best knowledge, no research on icebreaking by a free-rising buoyant body has been published. This is because the interaction among ice, body in free motion and water is very complex. On the other hand, it is interesting when the buoyant body breaks the ice plate most, or the optimal relative density of the body which can break the ice plate severest. A sphere is used as an example in the experimental and theoretical analysis.

2. EXPERIMENTAL METHODS

2.1 Ice Specimen Preparation

The ice plates in this study were made by freshwater in a cryostat at -20℃. The freshwater was boiled in order to maximize the removal of dissolved air in the water and to avoid the presence of bubbles. The boiled fresh water was placed in an EPS cylindrical container without a top cover, which ensure the heat transfer direction is in the same way as the growth direction of the ice crystal in reality. When the requirements of the thickness of the ice plates were met, the ice plates were removed from the container and moved into a cryostat at -5℃ for 10 hours. The diameter of ice plates was 345 mm and the thicknesses were 6 mm, 8 mm, and 10 mm respectively.

2.2 Experimental Setup

Figure 1 shows the experimental setup. The experimental facility can be divided into four systems: 1) the sphere location and releasing system; 2) the fixing system; 3) the supporting system; 4) the camera system. The properties of ice plate can be found in Ni et al. [6].

A sphere with a diameter of 112.5mm location and releasing system included a lift platform (in blue) and a releasing device (in yellow), as shown in Figure 1 (a) and (b). A supporter with a

groove was used for the ice fixing system. The detail was shown in Figure 1 (c). During the experiment, the ice plate was first put into the groove of the supporter, and then the fixed ring was covered over the ice plate, as shown in the enlarged view of Figure 1 (c), and finally the fixed ring was fixed with the supporter by four Clamps2. The ice fixing system was fixed with the water tank by eight Clamps1. The supporting system consisted of a square water tank and an outside shell frame. The size of the glass water tank was 0.6 m×0.6 m×0.6 m. The camera system included two high-speed cameras and four LED lamps. Placed on the horizontal surface, Camera 1 was in charge of capturing the motion trajectory of the floating sphere. Meanwhile, the destruction of the ice plate was captured by Camera 2 which was placed on the vertical surface.

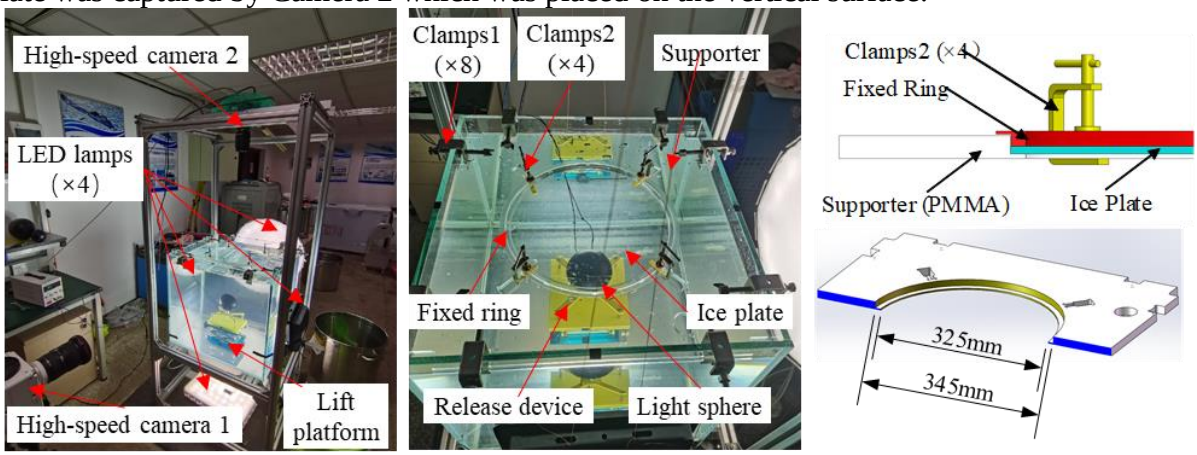

(a) (b) (c)

Figure 1. Experimental setup: (a) Supporting system and camera system. (b) Ice fixing system and sphere location and releasing system. (c) Cross-section diagram of ice fixing supporter and the fixation way of the ice plate.

3. RESULTS AND DISCUSSION

Through the experiment of the control variable method, four damage patterns were concluded as 'radial cracks (RCs)', 'radial cracks ⊕ circumferential cracks (RCs ⊕ CCs)', 'debris splashing' and 'ice plate breakup' patterns, with damage degree of ice plate rising.

To explores the effect of dimensionless density $\bar{\rho}$ on ice plate damage. Spheres with different dimensionless densities were used to break the ice plate with dimensionless thickness of the ice plate $\bar{h}$ = 0.089 and the dimensionless initial submergence depth of the sphere $\bar{L}_0$ = 2.31 constant.

Figure 2 shows typical pictures of the damage on the ice plate caused by spheres of different densities, at t' =0.1 s from bird's-eye view and horizontal view, respectively. From Figure 2 (a) to (c), it can be seen that with the increase of the relative density of the sphere, the damage state of the ice plate changes from 'debris splashing' to 'ice plate breakup' patterns; while from Figure 2(c) to (e), the damage state of the ice plate changes from 'ice plate breakup' to 'debris splashing' and then to 'RCs' patterns. To avoid randomness in the results, at least 10 repeated experiments were done for each density case. The failure mode of ice plate caused by spheres with different densities is shown in Figure 3. Because it was difficult to ensure the properties of each ice plate same exactly due to limits of icebreaking technology, different failure modes may appear at the same relative density. However, it was still reasonable to classify the damage degree of ice plates by statistical data of different failure modes.

Based on the results of previous experiments, 'ice plate breakup' pattern was severest in all the patterns. We took the probability of this pattern as a criterion and tried to link the damage degree of the ice plate with dimensionless kinetic energy $\bar{E}_{kt}$ and dimensionless momentum $\bar{M}_t$ of the sphere. As shown in the Figure 4, the dimensionless kinetic energy of the sphere achieves

the largest at $\bar{\rho}$ = 0.4, while the dimensionless momentum of the sphere achieves the largest at $\bar{\rho}$ = 0.6. Compared with the probability of ice breakup pattern, when the kinetic energy of the sphere is the largest, the probability of the ice plate breakup peaks (91.7%). From this point, it can be concluded that the kinetic energy of the sphere, rather than momentum, at the moment of collision dominates the damage degree of the ice plate. As a result, we adopt kinetic energy of the sphere at the moment of collision as a criterion for the icebreaking ability of a floating light sphere driven by net buoyant force hereinafter.

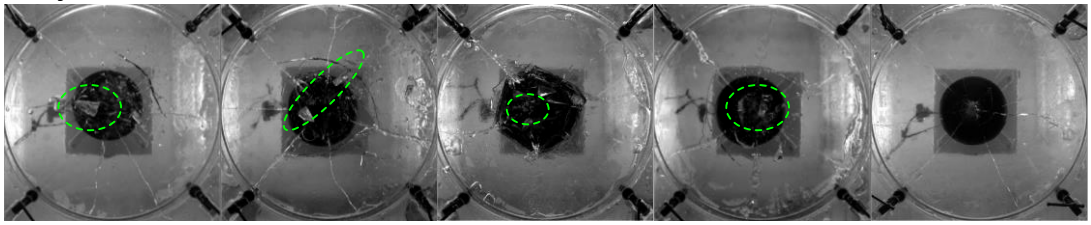

Bird's-eye view $(t' = 0.1\ \mathrm{s})$

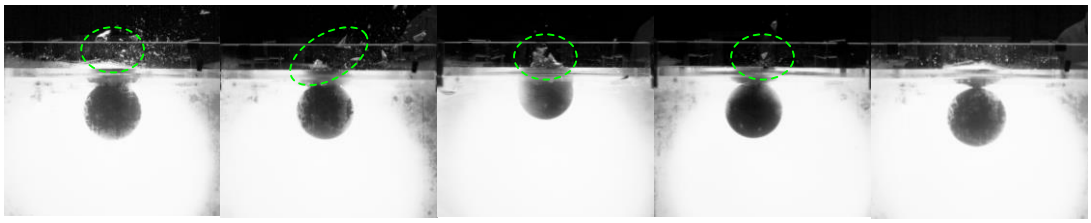

Horizontal view $(t' = 0.1\ \mathrm{s})$

(a) $\bar{\rho} = 0.146$ (b) $\bar{\rho} = 0.3$ (c) $\bar{\rho} = 0.4$ (d) $\bar{\rho} = 0.5$ (e) $\bar{\rho} = 0.8$

Figure 2. Destructiveness of ice plates caused by different relative densities of spheres from different views

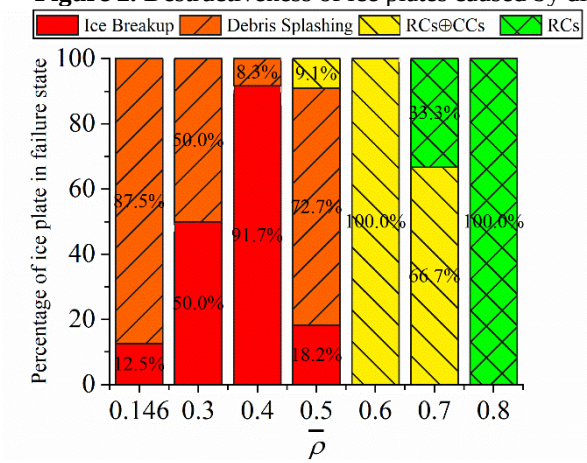

Figure 3. Probability of failure mode of ice plate impacted by spheres with different densities

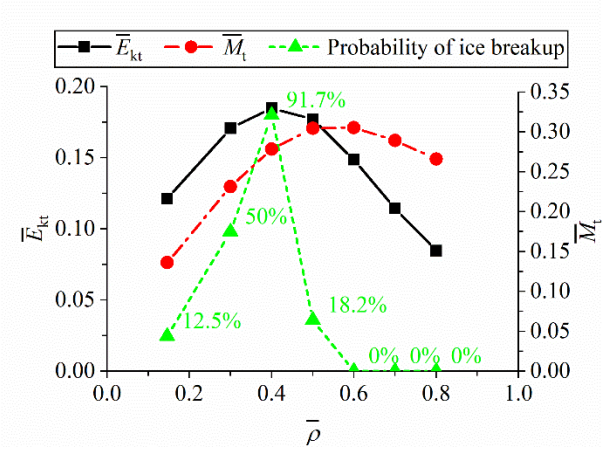

Figure 4. The relationship between $\bar{E}_{kt}$, $\bar{M}_t$ and the probability of the ice breakup with the relative density obtained in experiments.

4. MATHEMATICAL CONCLUSION

Driven by the buoyant force, a light sphere starts to accelerate from a resting position under the ice plate until it collides with the ice plate. A simplied theoretical force balance model was made as follows:

$$(m + m_a)\frac{dU}{dx}\cdot\frac{dx}{dt} = F_b - F_g - F_d \tag{1.1}$$

$$U\frac{dU}{dx}=\frac{-3C_d\cdot U^2+4Dg\left(1-\bar{\rho}\right)}{4D\left(\bar{\rho}+C_m\right)} \tag{1.2}$$

where m is the mass of the sphere; m_a is the added mass of the sphere; U is the velocity of the sphere; x is the displacement of the rising buoyant sphere; F_b is the buoyant force; F_g is the gravity force; F_d is the drag force; D is the diameter of the sphere; C_m is the added-mass coefficient. In this model, it was assumed that the drag coefficient C_d in the whole process was a constant to be determined. According to the simplified model, the relationship between $\bar{E}_{kt}$ and $\bar{\rho}$, $\bar{L}_0$, C_d is obtained. When $\partial\bar{E}_{kt}/\partial\bar{\rho}=0$, one can find $\bar{\rho}_{op}$. Figure 5 provides the change of $\bar{\rho}_{op}$ with $\bar{L}_0$ and C_d at a given C_m. It is found that $\bar{\rho}_{op}$ depends on the viscous effect of the fluid to a great extent. If the viscous effect is neglected, or for a non-viscous case, $\bar{\rho}_{op}$ equals to $\frac{\sqrt{3}-1}{2}$ identically. Otherwise, $\bar{\rho}_{op}$ declines along with the decrease of C_d at a given $\bar{L}_0$, and rises along with the increase of $\bar{L}_0$ at a given C_d, approaching to 0.5 for a very large $\bar{L}_0$ in the end.

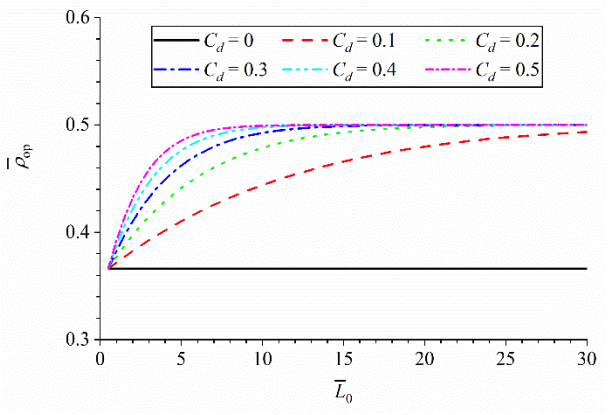

Figure 5. The relationship between $\bar{\rho}_{op}$ and $\bar{L}_0$ with different C_d

ACKNOWLEDGEMENT

This work is supported by the National Natural Science Foundation of China (Nos. 52192693，52192690，51979051 and 51979056), to which the authors are most grateful.

REFERENCES

[1] George, J. C., Clark, C., Carroll, G. M., Ellison, W. T. 1989. *Observations on the ice-breaking and ice navigation behavior of migrating bowhead whales (Balaena mysticetus) near Point Barrow, Alaska, spring 1985*. Arct. 42 (1), 24-30.

[2] Ren, H.; Zhao, X. 2022. *Numerical simulation for ice breaking and water entry of sphere*. Ocean Eng. 243, 110198.

[3] Wang, C.; Wang, J.; Wang, C.; Guo, C.; Zhu, G. 2021. *Research on vertical movement of cylindrical structure out of water and breaking through ice layer based on S-ALE method*. J. Theor App Mech-Pol, 53(11), 3110-3123.

[4] Ye, L. Y.; Guo, C. Y.; Wang, C.; Wang, C. H.; Chang, X. 2020. *Peridynamic solution for submarine surfacing through ice*. Ships Offshore Struct. 15(5), 535-549.

[5] M. Orlov and G. Bogomolov, 2016. *Study of the behavior of ice under shock and explosive loading*, In Proceedings of the 3rd Interna-tional Scientific Conference on Polar Mechanics, Vladivostok, Russia, Sept. 27–30, 192–202.

[6] Ni, B. Y.; Pan, Y. T.; Yuan, G. Y.; Xue, Y. Z. 2021. *An experimental study on the interaction between a bubble and an ice floe with a hole*. Cold Reg. Sci. Technol., 187, 103281.